IOSR Journal of Dental and Medical Sciences (IOSR-JDMS)
e-ISSN: 2279-0853, p-ISSN: 2279-0861.Volume 19, Issue 10 Ser.10 (October. 2020), PP 14-29
www.iosrjournals.org

Role of MRI in common and uncommon female pelvic masses: pictorial essay

Dr Shilpa Chudasama[1], Dr Daxa Khunt[2]
[1]*Associate Professor*
[2]*Resident*
Department of Radiodiagnosis, Shri M.P. Shah Government Medical College and
Shri Gurugobind Singh Government Hospital, Jamnagar.
Corresponding author: Dr Daxa Khunt
Resident, Department of Radiodiagnosis, Shri M.P.Shah Government Medical College and
Shri Gurugobind Singh Government Hospital, P.N.Marg, Jamnagar, Gujarat, India – 361008

Abstract
Background*: - The objective of this study was to evaluate role of Magnetic resonance (MR) imaging in the detection and staging of large pelvic masses and to assess usefulness and accuracy of MR imaging as compared to ultrasonography and CT scan in pelvic pathologies and assessment of their characteristics. Many large masses in the female pelvis arise from the reproductive organs (eg, uterus, cervix, ovaries and fallopian tubes). In addition, they may arise from the gastrointestinal system, urinary system, adjacent soft tissues, peritoneum, or retro-peritoneum or from metastases. The majority of large masses are uterine fibroid tumor, dermoid tumor, ovarian cyst, and ovarian cancer. Thus, the differential diagnosis for female pelvic masses is extensive. Establishing correct diagnosis and accurately staging of tumors is important, particularly when surgical resection can be option. In this article we illustrate MR imaging characteristics of various common and uncommon pelvic masses.*
Materials and methods*: - Detailed history of patient was obtained referred to radiology department for pelvic MRI or patient referred to MRI after Ultrasonography or CT scan of pelvis. All MRI were done with 1.5 Tesla simeans MRI Scanner using Axial T1WI, T2WI, fat sat and STIR; coronal and sagittal T 2 sequences, DWI images.*
Conclusions*: - the differential diagnosis for female pelvic masses is extensive and when large tumors, it may not always be possible to determine the site of origin to differentiate between tumors at imaging. Further Radiological imaging modality like transvaginal ultrasonography (TVS), CT scan have their limitation in case of very large lesion and of tissue characterization. For such case MRI is helpful. The application of MR imaging in pelvic masses goes beyond lesion detection to include assessment of disease staging.*
Key Words*; MRI, pelvis, uterus, adnexa, ovary, cervix*

Date of Submission: 09-10-2020 Date of Acceptance: 24-10-2020

I. Introduction

Female pelvic lesions are from uterus, cervix, ovaries, fallopian tubes, peritoneum or retro peritoneum.

Radiological imaging modality for female pelvis is transvaginal ultrasonography (TVS), CT scan and MRI. Among of them during routine radiological practice, TVS and CT scan have their limitation in case of very large lesion. TVS is difficult for evaluation of very large pelvic mass and CT scan has limitations if lesion has wide range of tissue discriminations. For such case MRI is helpful for evaluation of following: (a) Origin and extension (b) Tissue characterization (c) Relation with surroundings (d) Vascularity and invasion. It also Help for diagnosis of (a) Benign versus malignant (b) Staging of malignancy (c) Exact dimension (d) Operative planning. Additionally exact evaluation of vaginal lumen is possible by (Limited sequence MRI correlation done) with additional sequence of without and with gel introducing in vagina simple T2W sagittal and axial images are enough. An adnexal mass that appears suspicious at USG may be correctly diagnosed as a benign lesion at MR, preventing inappropriate radical surgery. MR is the most useful modality for evaluating adnexal lesions that are indeterminate at gray-scale ultrasound. However, MRI having Limitations like, Availability is limited, Costly as compare with TVS and CT scan, Time consuming and many contraindications like claustrophobia and operative patient.

II. Materials and Methods

This prospective study was conducted at the Department of Radiodiagnosis, M. P. Shah govt. medical college and Shri Guru gobind Singh Government Hospital, Jamnagar, Gujarat during MAY 2018 to MAY 2020. After taking informed consents of patients presenting to radiology department for examination of MRI pelvis directly or referred to MRI center after being done with ultrasonography and/or CT scan for evaluation of pelvic pathology. Detailed history of patient including menstrual history and findings of gynaecological examination were taken into consideration and assessed with 1.5 Tesla Magnetic Resonance Imaging system. All patients were of age ranging in between 15 years to 70 years.

Inclusion criteria:
1. Confirmed cases of pelvic pathology came for better imaging evaluation.
2. Suspected cases pelvic pathology.
3. Cases of all age groups of female.

Exclusion criteria:
1. Male patient.
2. Pathology other than pelvic origin
3. Post treatment patient
4. Cardiac pacemaker.
5. Claustrophobia.
6. Patients who are unwilling for imaging**.**

Protocol:
After enrolment of the case and detailed history, MRI pelvis were done by 1.5 Tesla Magnetic Resonance Imaging system (Magnetom Essenza, Siemens health care, Germany) using Axial T1WI, T2WI, fat sat and STIR; coronal and sagittal T 2 sequences, DWI images..

Result: Following pathologies are noted.

Uterine pathology

Endometrial Cancer

Endometrial cancer is the fourth most common malignancy in females and the most common malignancy of the female reproductive tract. Approximately 75% of cases occur in postmenopausal women with the median age at diagnosis being 70 years. Adenocarcinomas account for 90% of endometrial neoplasms. The most common clinical manifestation is abnormal vaginal bleeding. (1, 2) The staging of endometrial carcinoma is based on extension of the primary tumor, adenopathy, and metastases. MR imaging is useful not only in identifying the tumor but also in assessing myometrial invasion, adenopathy, and metastases. These tumors have intermediate to low signal intensity on T1-weighted MR images and low signal intensity on T2-weighted images. On contrast-enhanced MR imaging, it enhances less than myometrium; on delayed scans, there is less distinction in enhancement (3, 4). MR imaging has been reported to be helpful in the staging of endometrial cancer. MR imaging is helpful in cancer staging. Tumors are staged on the basis of depth of myometrial invasion. The presence of myometrial invasion is indicated by loss of the normal endometrium-myometrium interface. The differential diagnosis for endometrial cancer may include cervical cancer, endometrial polyps, and mesenchymal tumors of the uterus. Distinguishing between these entities is easier in smaller tumors.

Endometrial polyps

Endometrial polyps are a common cause of postmenopausal bleeding. These are benign nodular protrusions of the endometrial surface. The polyp may be broad-based and sessile or pedunculated. Although endometrial polyps may be visualized at transvaginal US as nonspecific endometrial thickening or focal masses within the endometrial canal. Polyps are best seen at sonohysterography and appear as echogenic, smooth, intracavitary masses outlined by fluid (5). Cystic spaces corresponding to dilated glands filled with proteinaceous fluid may be seen within the polyp. The point of attachment should not disrupt the endometrial lining. Polyps may also be seen at hysterosalpingography as pedunculated filling defects within the uterine cavity or at T2-weighted MR imaging as low signal-intensity intracavitary masses surrounded by high-signal-intensity fluid and endometrium. Because of its excellent soft-tissue contrast resolution and multiplanar capability, magnetic resonance imaging (MRI) can demonstrate morphologic features and the extent of lesions, both of which are useful in making decisions for surgical or hysteroscopic resection. Color Doppler US may be used to image vessels within the stalk. Fibroids or foci of endometrial hyperplasia or carcinoma can mimic a sessile polyp, and foci of atypical hyperplasia are sometimes found within polyps (6).

Fibroids

Uterine leiomyoms are benign soft-tissue tumors that occur in patients of all ages. Intra-uterine leiomyoma can be intramural (mc) common, sub serosal and submuosal (least common) and extra-uterine leiomyoma can be broad ligament leiomyoma, cervical or parasitic leiomyoma They are commonly identified at US as hypoechoic solid masses, but they may be heterogeneous or hyperechoic, depending on the degree of degeneration and calcification. T1- weighted MR imaging, fibroids appear iso- to hypointense relative to the myometrium, whereas at T2-weighted imaging they appear homogeneously hypointense or heterogeneously hyperintense when degeneration is present. (7) fibroids that have undergone cystic degeneration/necrosis can have a variable appearance, usually appearing high signal on T2 sequence. Giant fibroids are known to arise from the uterus, but occasionally from the broad ligament also. on Ultrasound, seen as a hypoechoic, solid, well-circumscribed adnexal mass, although that can be heterogeneous when large amd generally no interface between the tumor and uterus and no straight relation to the ipsilateral ovary. On contrast MRI most enhance similarly to the myometrium while larger leiomyomas tend to enhance less and heterogeneously. (8,9) Differential diagnosis of Leiomyoma involving the broad ligament is pedunculated subserosal leiomyoma projecting towards the broad ligament, solid ovarian neoplasms (with dominant fibrous components) like ovarian fibroma or fibrothecoma and Brenner tumor: which are inseparable from the ovary, neurofibroma in the pelvis. (10)

Gestational Trophoblastic Disease

Gestational trophoblastic disease encompasses a broad spectrum of conditions, includes hydatidiform mole, invasive mole, choriocarcinoma, and placental site trophoblastic tumor. Although sonography is the examination of choice for the initial diagnosis, MR imaging has a role in the detection of gestational trophoblastic disease and the evaluation of the extent of its complications [11,12].

Hydatidiform Mole

Hydatidiform mole constitutes 80% of cases of gestational trophoblastic disease. It can be partial or complete. Ultrasonography (US) is the modality of choice for initial diagnosis of hydatidiform mole The performance of US in diagnosing molar pregnancies is surprisingly poor due to the difficulty in differentiating partial hydatidiform mole from nonmolar abortion and retained products of conception. While GTN after a molar pregnancy is usually diagnosed with serial β-hCG titers, imaging plays an important role in evaluation of local extent of disease and systemic surveillance.

US findings suggestive of PHM include (a) empty gestational sac or one containing amorphous echoes representing fetal parts; (b) elongated or ovoid gestational sac (c) fetal demise, anomalies, or growth restriction; (d) oligohydramnios; and (e) enlarged placenta relative to the size of the uterus with internal cystic change producing a “Swiss cheese pattern” (13, 14). Differentiating between PHM and CHM carries prognostic significance because of the higher rate of postmolar GTN in CHM compared with PHM. In complete mole findings are of enlarged uterus and intrauterine mass with cystic spaces without any associated fetal parts, multiple cystic structures classically give a "snowstorm" or "bunch of grapes" type appearance. Multiple large, bilateral, functional ovarian cysts called theca lutein cysts are seen in less than 20% of cases of CHM (5) and result from ovarian stimulation by the high level of β-hCG (15). CT is used to stage a suspected malignancy and evaluate for metastatic disease in cases of GTN. On T2-weighted images, a complete mole appears as a heterogeneous mass of high signal intensity that distends the endometrial cavity. Numerous cystic spaces may be present in the mass [16]

Invasive mole

An invasive mole develops in approximately 10% of patients after molar evacuation and infrequently after other gestations. This defined as a mole which penetrates and may even perforate the uterine wall. There is invasion of the myometrium by hydropic chorionic villi, accompanied by proliferation of trophoblast. The tumor is locally destructive and may invade parametrial tissue and blood vessels [12]. An invasive mole appears as a poorly defined mass displaying mixed signal intensity on T2-weighted images and deeply invades the myometrium. Complete or partial disruption of the junctional zone may also be seen. On T1-weighted images, the mass is isointense to the myometrium with scattered foci of high signal intensity because of the presence of hemorrhage. Molar like structures appear as tiny cystic lesions within the well-enhanced zone of trophoblastic proliferation in a mass of the invasive mole. With the penetration of the tumor into the myometrium, the invasive mole appears as a more aggressive entity than does choriocarcinoma [12,16]

Cervical tumor

The minimal deviation adenocarcinoma (so-called adenoma malignum) is a rare type of malignant epithelial tumor that affects the uterine cervix. Using magnetic resonance imaging (MRI), minimal deviation adenocarcinoma appears as a multicystic mass with solid components in the deep cervical stroma (17,18). Some well-differentiated adenocarcinomas with tubular glands can also appear as multicystic masses in the cervical stroma. Furthermore, some benign conditions that affect the uterine cervix may also have multicystic features (4 ,9). Nabothian cysts usually resemble minimal deviation adenocarcinoma (7) While some reports claim that the MRI characteristics of minimal deviation adenocarcinoma or adenocarcinoma can be used to differentiate these from benign lesions, some authors report that differentiation with MRI is impossible However, although minimal deviation adenocarcinoma is an extremely well-differentiated adenocarcinoma, the prognosis is unfavourable. (17, 18, 19).

Adnexal masses

Adnexal masses are classified into three groups: cystic masses (unilocular or multilocular), cystic and solid masses, and predominantly solid masses. MR imaging allows differentiating malignant from benign tumors. MR imaging criteria for malignant ovarian tumors are (a) a solid mass or large solid component, (b) wall thickness greater than 3 mm, (c) septal thickness greater than 3 mm and/or vegetations or nodularity, and (d) necrosis. The ancillary criteria were also formulated as (a) involvement of pelvic organs or the sidewall; (b) peritoneal, mesenteric, or omental disease; (c) ascites; and (d) adenopathy. (20, 21, 22).

Cystic Masses

Cystic masses include nonneoplastic cysts, benign neoplasms, and borderline neoplasms. Functional cysts, paraovarian cysts, hydrosalpinx, endometriotic cysts, serous cystadenomas, mucinous cystadenomas, and mucinous cystic tumors of borderline malignancy.

Unilocular Cystic Masses: Functional cysts, paraovarian cysts, hydrosalpinx, and serous cystadenomas usually appear as unilocular cystic masses. They are well-circumscribed cystic masses. When uncomplicated, they have low signal intensity on T1-weighted images and high signal intensity on T2-weighted images.

Hydrosalpinx: when large enough—may also mimic a cystic ovarian tumor., dilated fallopian tubes appear as fluid-filled structures that are sausage-shaped and/or C- or S-shaped when viewed in multiple planes. Salpingitis and pelvic endometriosis are common causes of hydrosalpinx because they often obliterate the fimbriated end of the fallopian tube. (22)

Serous tumors: common and account for approximately 25% of benign ovarian neoplasms . Bilaterality is frequent, occurring in 12%– 23% of cases . Serous cystadenomas are composed of unilocular or multilocular cysts filled with clear watery fluid. The lining of the cyst is flat or may have small papillary projections. The typical MR imaging appearance of serous cystadenoma is a unilocular cyst with a thin wall (23).

Multilocular Cystic Masses : includes Endometriotic cysts, mucinous cystadenomas, and mucinous cystic tumors of borderline malignancy, tubo-ovarian abscess

Tubo-ovarian abscess: patients with present with fever and abdominal pain, and the diagnosis is usually made clinically or with transvaginal US. MR imaging may demonstrate the abscess as a high-signal-intensity mass on T1-weighted images when its contents are complicated. Strong perilesion enhancement of a thick wall is consistent with a tubo-ovarian abscess (22,24).

Mucinous tumors: common and account for approximately 41% of benign ovarian neoplasms (25). In contrast to serous tumors, only 2%–5% of cases are bilateral. Mucinous cystadenomas are large multilocular cysts containing gelatinous material or fluid of various viscosity. Therefore, the loculi of the tumors often show various signal intensities on both T1- and T2- weighted images and a so-called “stained glass” appearance (26). They rarely appear as unilocular cysts.

Cystic and Solid Masses

Cystic and solid mass strongly supports the diagnosis of ovarian malignancy. Primary epithelial carcinomas, metastatic tumors Mature cystic teratoma often show a cystic and solid appearance. is the important exception to this appearance and is also described in this section.

Metastases to the ovaries are another important group of ovarian carcinomas. Extragenital tumors of the intestines, stomach, and breast commonly metastasize to the ovaries. They spread via blood vessels and lymphatics. appearances of metastatic tumors are cystic and solid masses.(22)

Mature cystic teratoma is the most common ovarian tumor, accounting for 20% of all ovarian neoplasms (27). Histologically, cystic teratomas are composed of a cyst lined by epithelium containing sebaceous and sweat glands. Tissue from all three germ layers is present, with ectoderm predominating (28). MR imaging demonstrates the fatty material as a high-signal-intensity component paralleling that of subcutaneous fatty tissue on T1-weighted and fast spin-echo T2-weighted images. The cyst shows chemical shift artefact (28,29,30). A selective chemical fat suppression technique enables differentiation of cystic teratomas from hemorrhagic adnexal processes (29,30) Other MR imaging findings include layering or floating debris, soft-tissue protuberances (Rokitansky nodules or dermoid plugs), and low-signal-intensity teeth. Malignant transformation is rare.

Solid Masses

Predominantly solid ovarian masses include benign, borderline, and malignant tumors. Fibrothecomas, Brenner tumors, granulosa cell tumors, and dysgerminomas.

Fibrothecoma are the most common solid benign tumors of the ovary and rarely malignant. They composed of spindle, oval, or round cells forming variable amounts of collagen. Because of these intersecting bundles of spindle cells, collagen, and hyalinized tissue, fibromas show predominantly low signal intensity on T2-weighted images and intermediate signal intensity on T1-weighted images (31) On the other hand, edema and cyst formation are relatively common pathologic findings in the tumor. Therefore, fibrothecomas can show mixed low to high signal intensity on T2-weighted images (31). The differential diagnosis includes nondegenerated subserosal uterine leiomyomas.

Most Brenner tumors are benign, accounting for 4%–5% of benign surface epithelial–stromal tumors (32). The abundant fibrous content and calcification in the tumor result in extensive low signal intensity on T2-weighted images (33,34). Brenner tumors are reported to show lower signal intensity on T2-weighted images than other solid tumors (33,34). Brenner tumors have a frequent association with mucinous cystic tumors in the same ovary. Malignant Brenner tumors (transitional cell carcinomas) are extremely rare and they have cystic and solid appearances at gross examination. Intravenous administration of gadolinium contrast material is not essential for characterization of fibromas or Brenner tumors when the signal intensity of the tumor is typical.

Epithelial ovarian carcinomas may appear predominantly solid. Specifically, serous carcinomas are sometimes solid (24). Metastatic ovarian carcinomas, especially krukenberg tumors may have a predominantly solid appearance (35,36).

Peritoneal inclusion cyst

Also known as peritoneal pseudo cysts and inflammatory cysts of the pelvic peritoneum, present with a variety of imaging appearances, which can be confused with various adnexal masses of the female pelvis. It occur almost exclusively in premenopausal women with a history of previous abdominal or pelvic surgery, trauma, pelvic inflammatory disease, or endometriosis [37,38].

It range in size from several mm in diameter to bulky masses that may fill the pelvis and abdomen. Peritoneal fluid accumulation within adhesions appears as complex multicystic adnexal masses on sonography. Imaging Characteristics includes Spider Web Pattern (Entrapped Ovary) Peritoneal adhesions extend to the surface of the ovary and may distort the ovarian contour but do not penetrate the ovarian parenchyma (39). The entrapped ovary appears like a spider in a web. Sometimes, the ovary may be eccentrically located to the adhesions. On imaging, it appears as extremely irregular in shape and reflect the invaginations of surrounding structures in the cyst wall because pseudocysts have no true walls (walls are formed by surrounding organs) [40]. On MR imaging, peritoneal inclusion cysts have low signal intensity on T1-weighted images and high signal intensity on T2-weighted spin-echo images, suggesting that the fluid is serous.

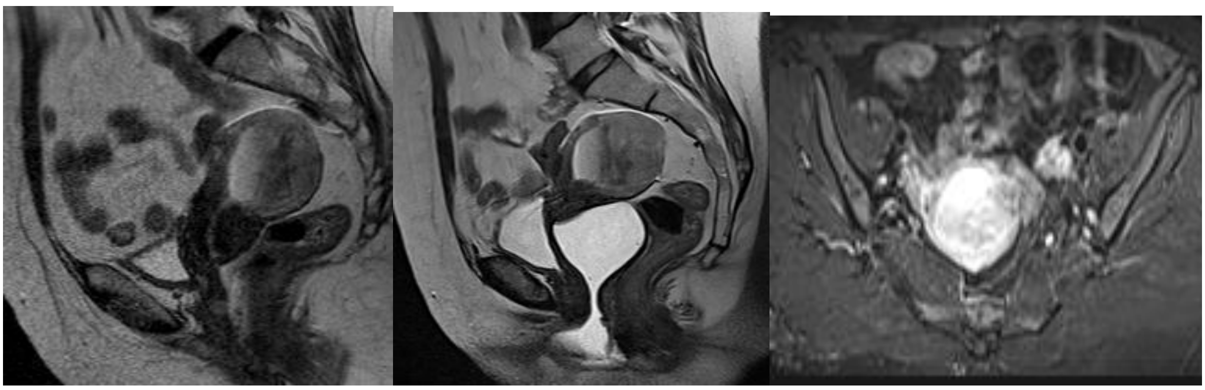

T2 SAG T2 SAG (with jelly) STIR

Endometrial carcinoma in 60 year old female with complain of post-menopausal bleeding (a) sagittal unenhanced T2WI without jelly (b) sagittal unenhanced T2WI with jelly shows heterogeneously hyperintense lesion arising from endometrium associated with fluid collection within endometrial cavity (C) STIR image shows ill-defined solid heterogeneously hyperintense lesion.


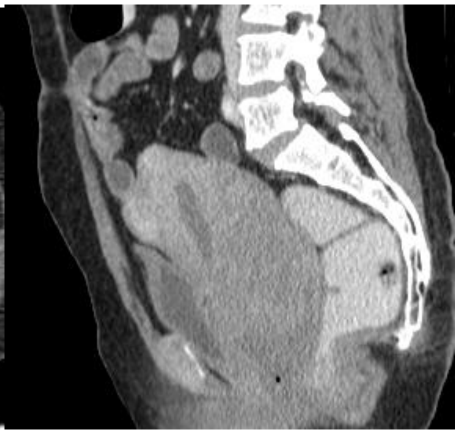

CECT axial CECT sag

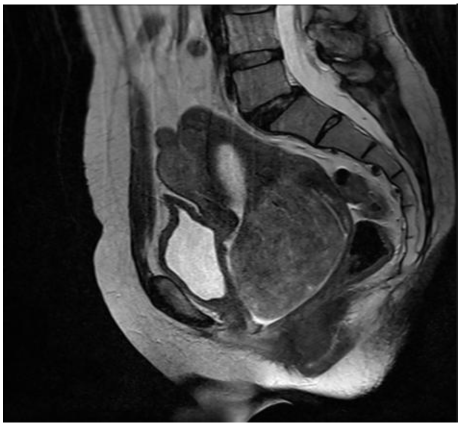
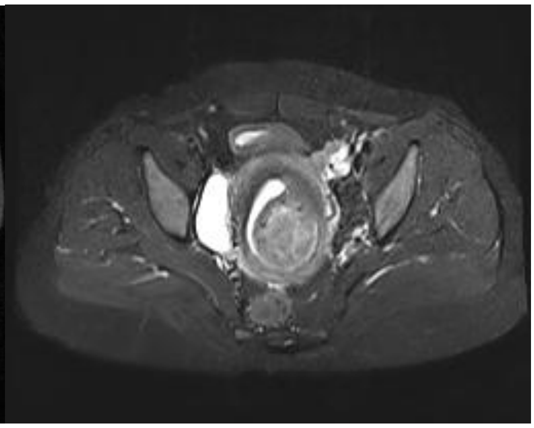

T2 SAG STIR axial

Endometrial polyp in 52 year old female with complain of bleeding per vgina. CECT (a) axial and (b) sagittal images show heterogeneously enhancing soft tissue density polypoidal lesion within cervical canal possibly arising from uterus. (c) sagittal unenhanced T2WI (d) axial unenhanced STIR image shows better visualisation polypoidal lesion within cervical canal arising from posterior uterine wall through stalk. MRI images shows better visualisation of stalk.


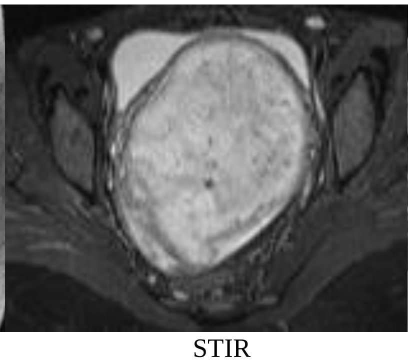
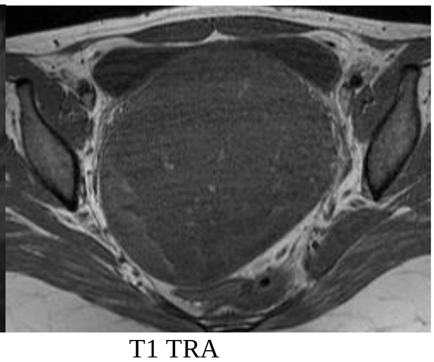

T2 SAG STIR T1 TRA

Endometrial polyp in 39 year old female with complain of lower abdominal pain associated with menorrhagia (a) sagittal unenhanced T2WI (b) axial unenhanced STIR image shows well-defined heterogeneously hyperintense polypoidal lesion within upper part of vagina arising from fundus of uterus through a stalk (C) On TIWI it appears hypointense. Further histo-pathological examination done on which malignant transformation proved.

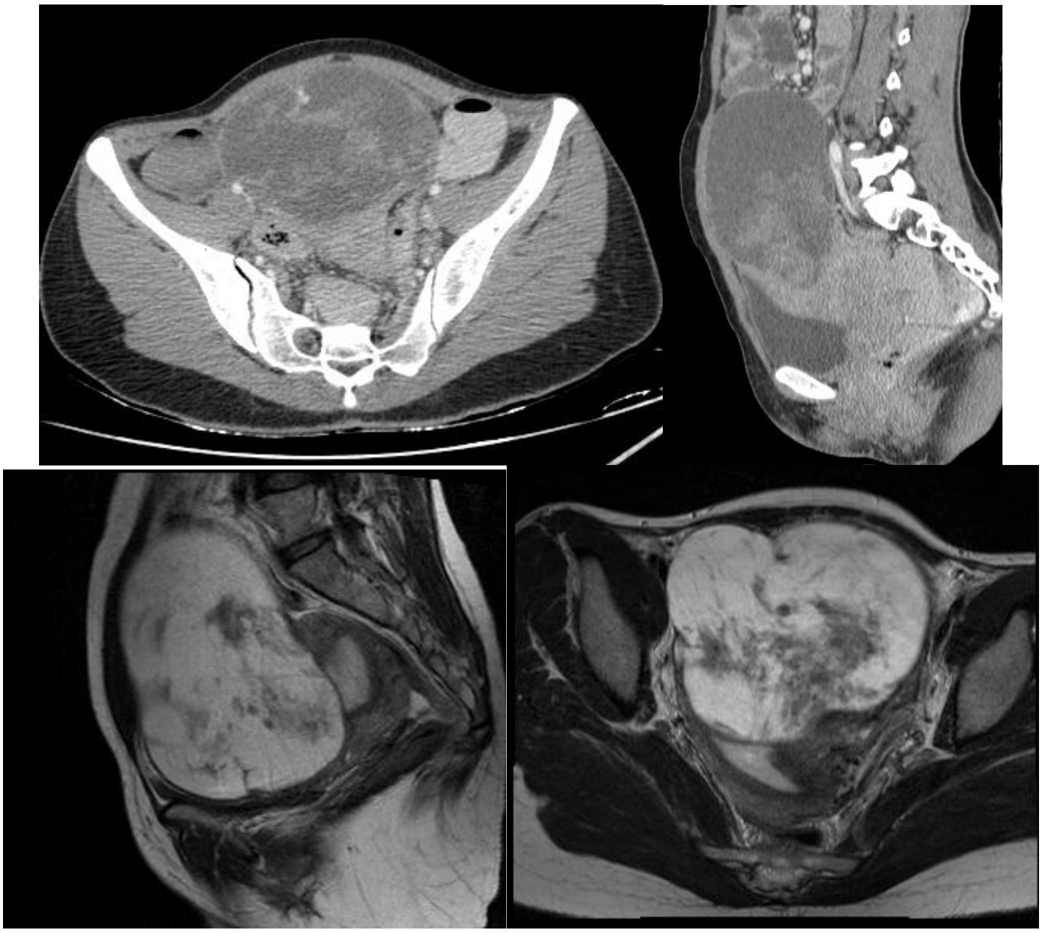

- Uterine fibroid with internal degenerative changes in 34 year old female with complain of lower abdominal pain (a)contrast enhanced CT axial and (b)sagittal images show large, solid cystic lesion arising from fundo-anterior wall of uterus, (c) unenhanced T2WI axial and (d) sagittal images shows better characterisation of mass, which appears heterogeneously hyperintese, suggestive of fibroid with arising from fundoanterior wall of uterus with internal degenerative changes.
-

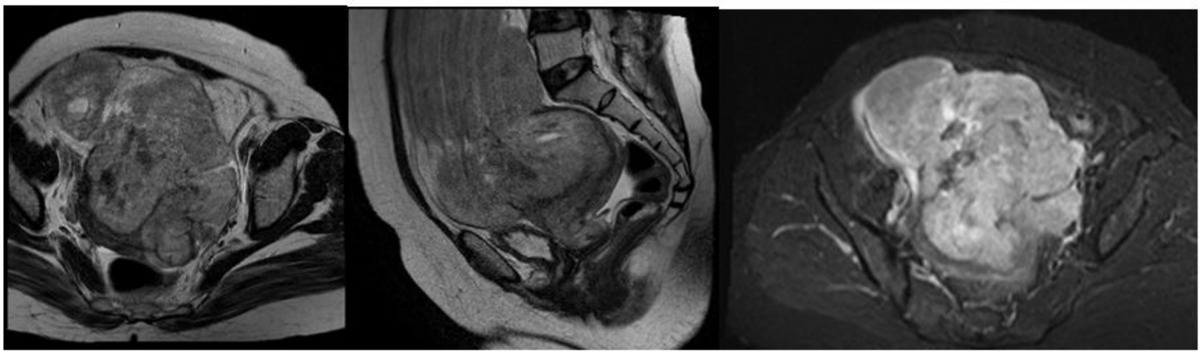

Large lobulated fibroid in 60 years old female having complain of lower abdominal pain (a) unenhanced T2WI axial (b) unenhanced T2WI sagittal; and (c) STIR axial images show multilobulatd altered signal intensity mass lesion arising from uterus. similar characteristic lesion is noted arising from left lateral wall of uterus. On histopathology fibroid was confirmed.

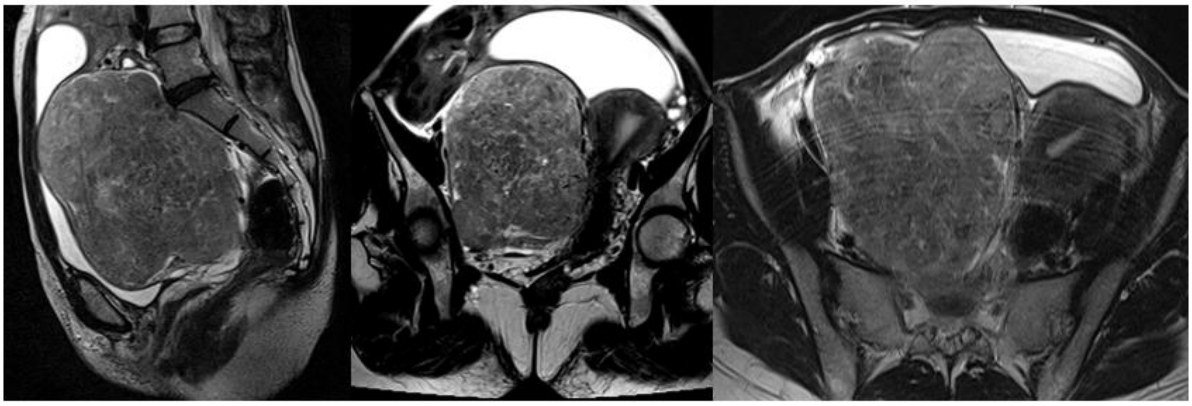

T2 SAG T2 COR T2 TRA

Right sided broad ligament fibroid in 35 year old female with complain of painless abdominal distension (a) sagittal unenhanced T2WI (b) coronal unenhanced T2WI and (c) T1WI axial images shows hypointense lesion on right side of uterus with few areas of hyper-intensity within lesion, suggestive of degenerative changes in fibroid.

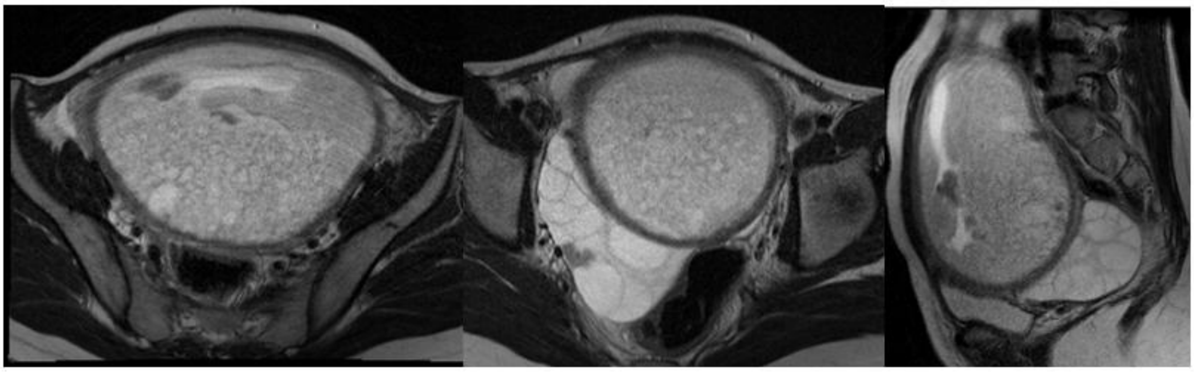

T2 axial T2 axial T2 SAG

Complete hydatidiform mole in 32 years old female patient with complain of 5 months of amenorrhea, UPT positive status with lower abdominal pain and bleeding per vaginum. (a) axial unenhanced T2WI and (b) sagittal unenhanced T2WI images show heterogeneous heterogeneous mass of high signal intensity distending the endometrial cavity with multiple tiny cystic spaces present in the mass and no evidence of fetal par noted. Also there is bilateral enlarged ovary with theca lutein cysts noted which develops in response to high levels of ß-human chorionic gonadotropin.

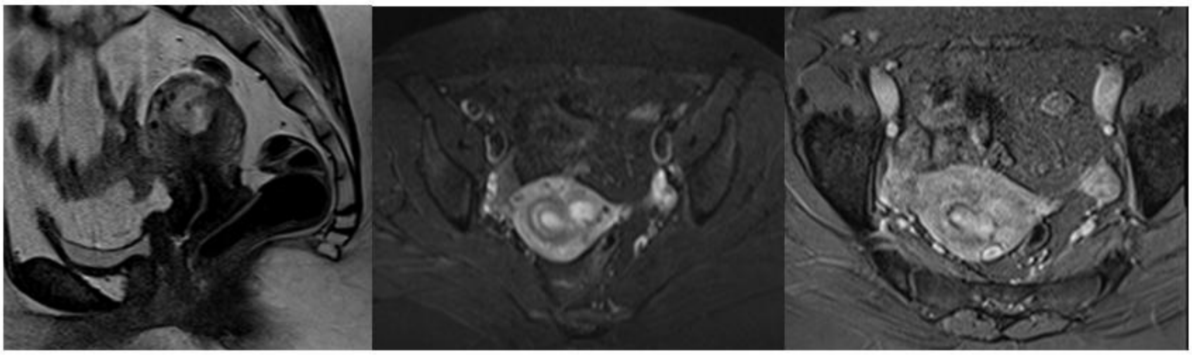

T2 SAG STIR axial GRE

Invasive hydatidiform mole in 30 years old female patient with complain of 4 months of amenorrhea, UPT positive status with lower abdominal pain. (a) sagittal unenhanced T2WI and (b) STIR axial image shows heterogeneous intensity lesion involving fundal part of endometrial cavity (C) GRE image shows no blooming.

on USG correlation structure with internal echogenic content was noted involving endometrial cavity with no evidence of FCP.

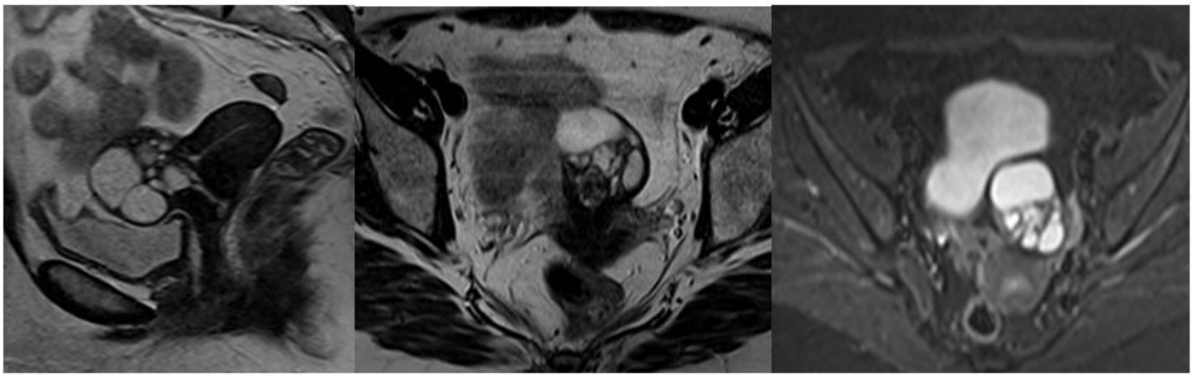

T2 SAG T2 TRA T1 TRIM TRA

Cervical minimal deviation adenocarcinoma (MDA) in 43 year old female with complain of watery vaginal discharge, (a) sagittal unenhanced T2WI (b) axial unenhanced T2WI and (c) axial STIR images shows exophytic solid cystic (predominantly cystic) lesion arising from anterior wall of cervix appears predominantly hyperintense on T2WI and on STIR.

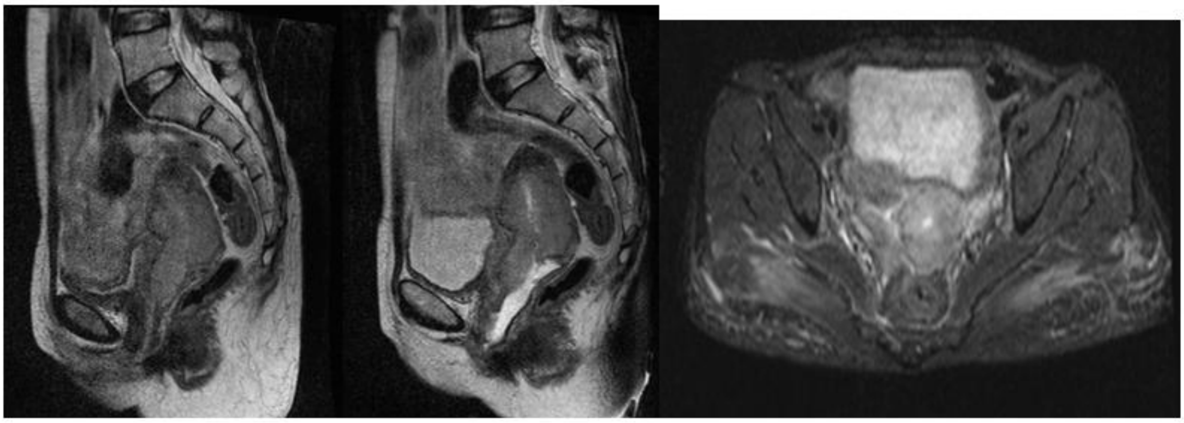

Cervical carcinoma in 56 years old female having complain of post-menopausal bleeding, (a) Non enhanced T2WI sagittal without jelly and (b) with jelly images shows an mildly hyper intense lesion like thickening of involving cervix (anterior lip >posterior lip) causing narrowing of cervical canal with resultant fluid collection within endometrial cavity. (c) STIR axial images shows hyperintense thickening Superiorly, it extends to endometrium with its irregularity, anteriorly lies in close approximation with posterior wall of urinary bladder associated with its thickening and inferiorly, extends into upper 1/3rd of vagina.

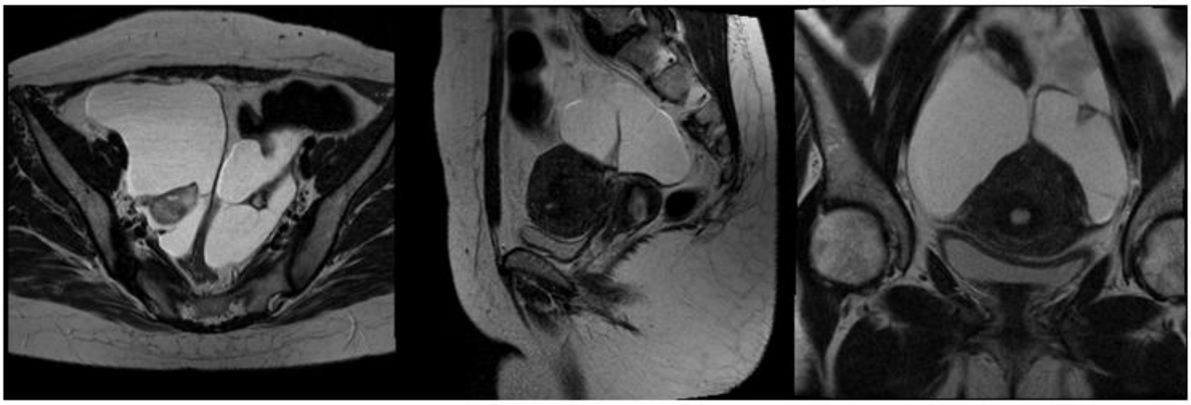

T2 TRA T2 SAG T2 cor

Bilateral hydro-salpinx in 30 year female with complain of lower abdominal pain, aggravating during menstruation (a) axial unenhanced T2WI (b) sagittal unenhanced T2WI and (c) coronal unenhanced T2WI shows tortuous hyperintense cystic lesion with incomplete septa in bilateral adnexa.

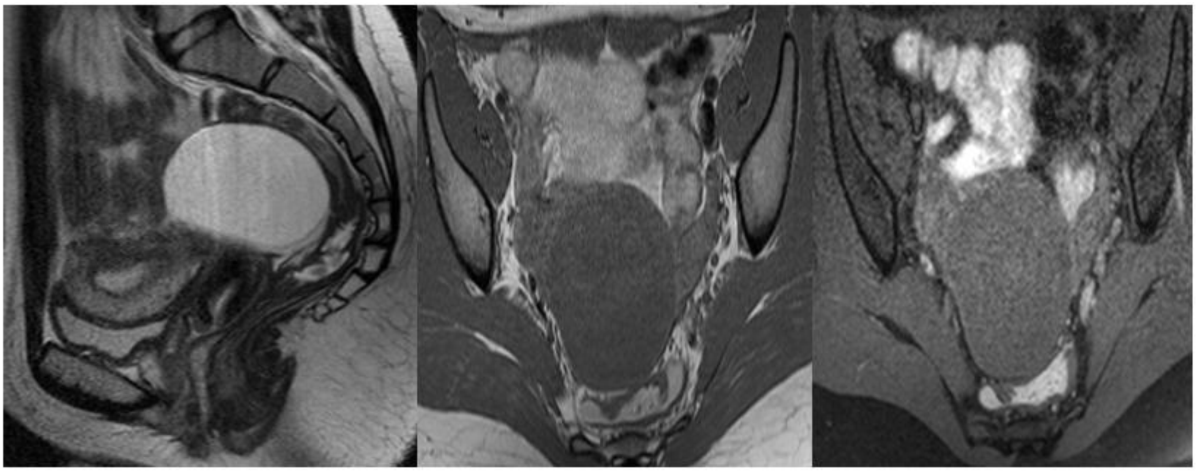

T2 SAG T1 TRA T1 FS TRA

Right ovarian unilocular serous cyst adenoma in 18 year old female with complain of lower abdominal pain (a) sagittal unenhanced T2WI shows hyperintense cystic lesion (b) axial unenhanced T1WI and c) T1 FS axial images shows hypointense lesion

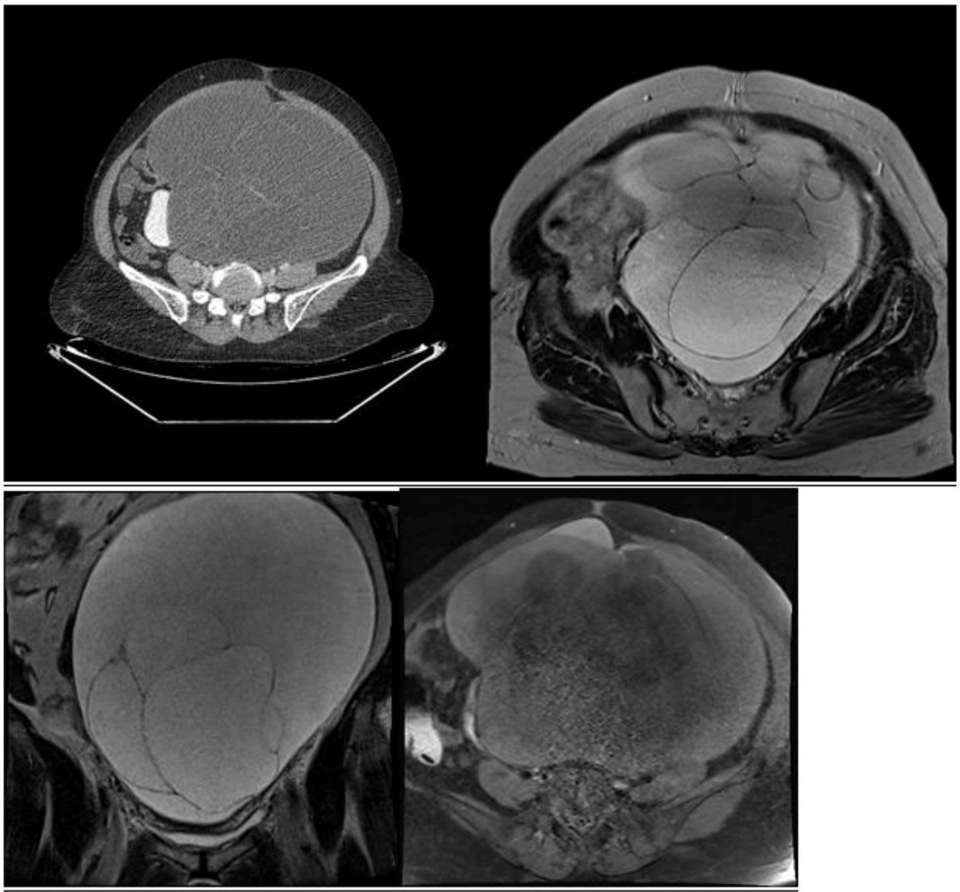

Right ovarian mucinous cyst adenoma in 40 year old female with complain of abdominal distention, pain associated with bilateral pedal edema (a) axial CECT abdomen shows large thin walled cystic lesion with internal septa arising from pelvic cavity and reaching upto epigastric region and causing compressive effect on surrounding structure. On (b) axial unenhanced T2WI and (c) coronal T2WI, it appears hyper intense with fine internal septa and arising from left ovary. (d) On axial unenhanced T1WI image it appears heterogenously hypointense. Heterogeneous signal intensity is due to mucin component.

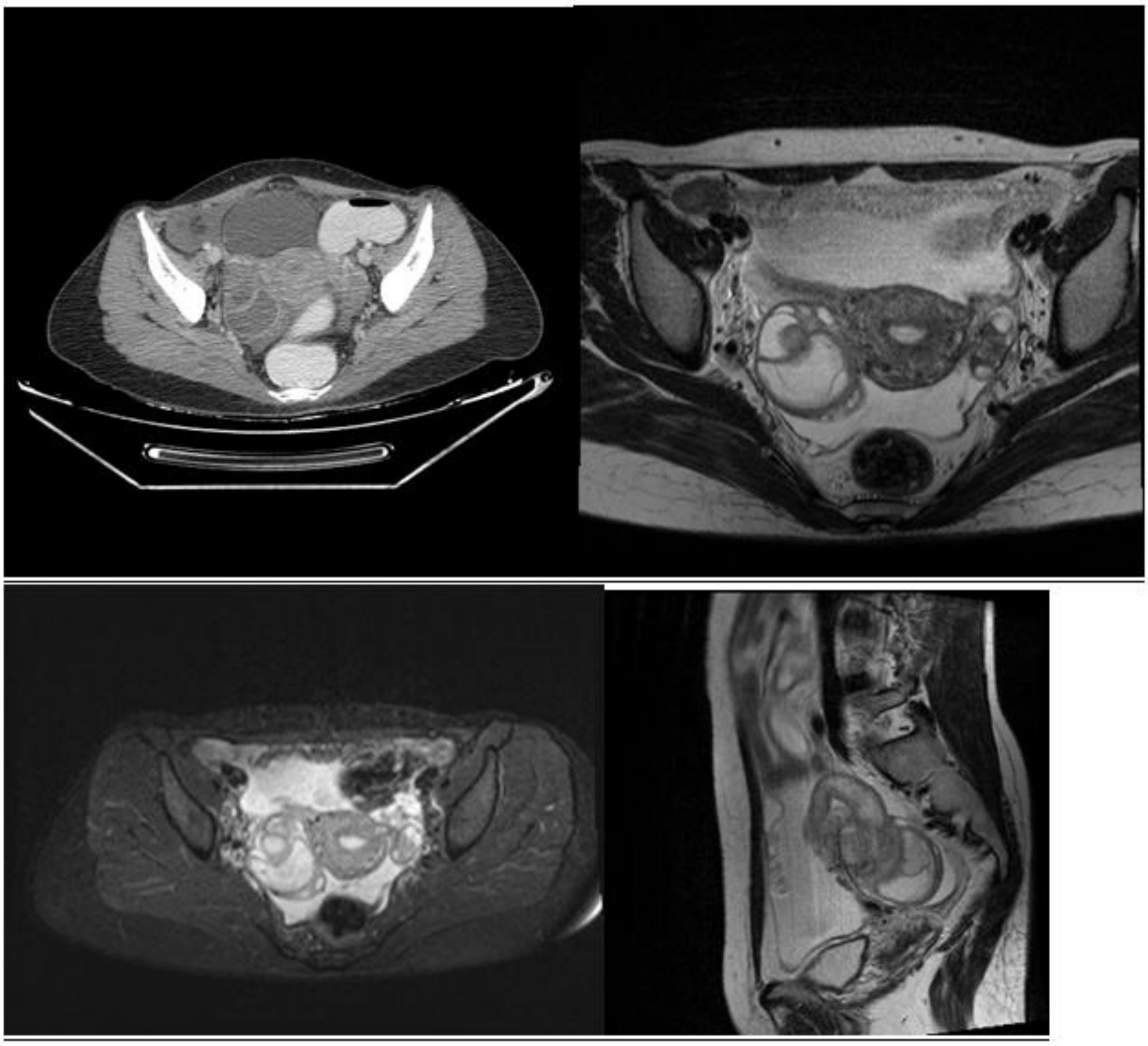

Right sided tubo-ovarian complex with pyo-salpinx in 30 years old female having complain of lower abdominal pain associated with weight loss. (a) axial unenhanced CT images shows peripherally enhancing multiloculated cystic lesion which show inter-communicating tubular structures involving right adnexa and right ovary cannot be separately visualised from lesion. (b) axial unenhanced T2WI, (c) STIR unenhanced T2WI and (d) sagittal unenhanced T2WI images allows better visualisation of tubo-ovarian complex and pyo-salpinx which appears heterogeneously hyper intense. Note mild ascites also.

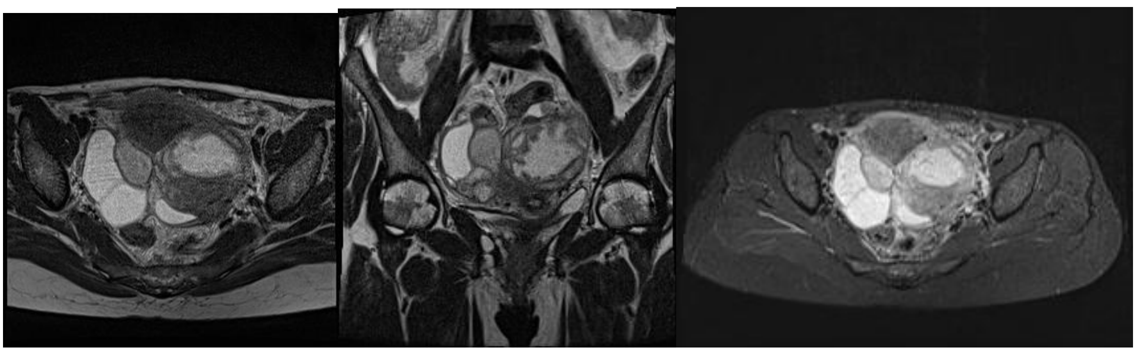

Bilateral tubo-ovarian abscesses in 35 years old female having Complain of pain in abdomen with fever and decreased appetite and WBC count was 21,000 cu/mm. (a) unenhanced T2WI axial (b) unenhanced T2WI sagittal; and (c) STIR axial images show multi-loculated heterogeneously hyper-intense cystic lesions involving bilateral adnexa with bilateral ovaries cannot be separately visualised from lesions.

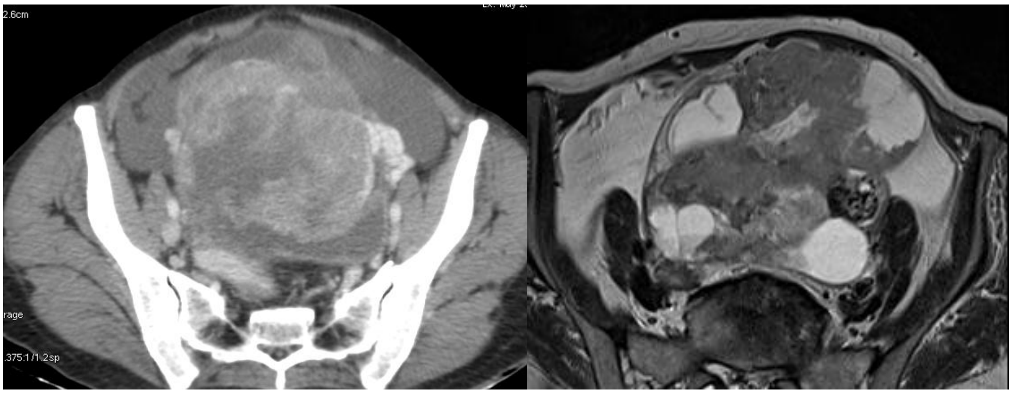

CECT axial T2 TRA

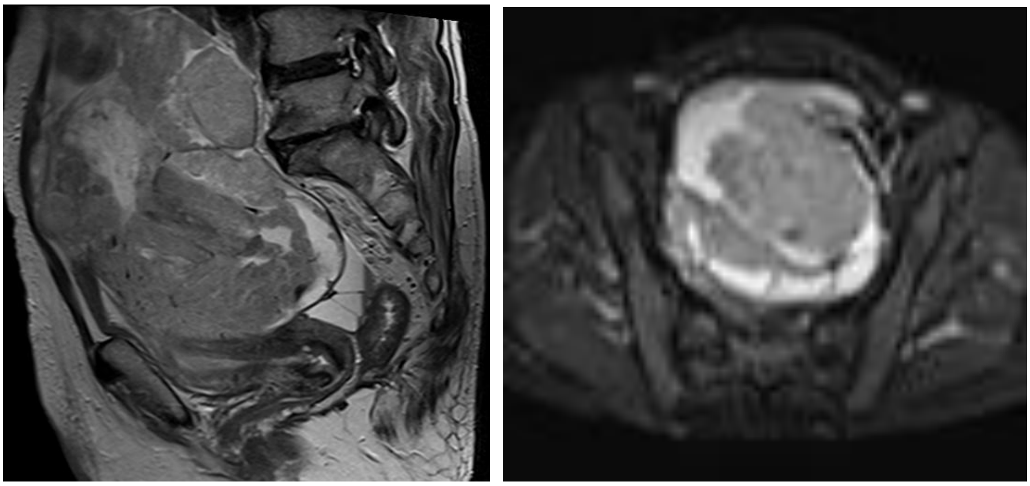

T2 SAG T1 TRIM

Right ovarian malignant mass lesion in 65 year old female with complain of lower abdominal pain, weight loss, difficulty in passing urine and constipation (a) contrast enhanced CT images shows heterogeneously enhancing lesion involving pelvic cavity which causes mass effect in form of extra luminal compression over uterus inferiorly, further more for better evaluation on non-contrast MRI pelvis images (b) sagittal unenhanced T2WI (c) axial unenhanced T2WI and (d) axial STIR images shows large solid cystic heterogeneous intensity lesion arising from right ovary and it allowed visualization of left ovary separately.

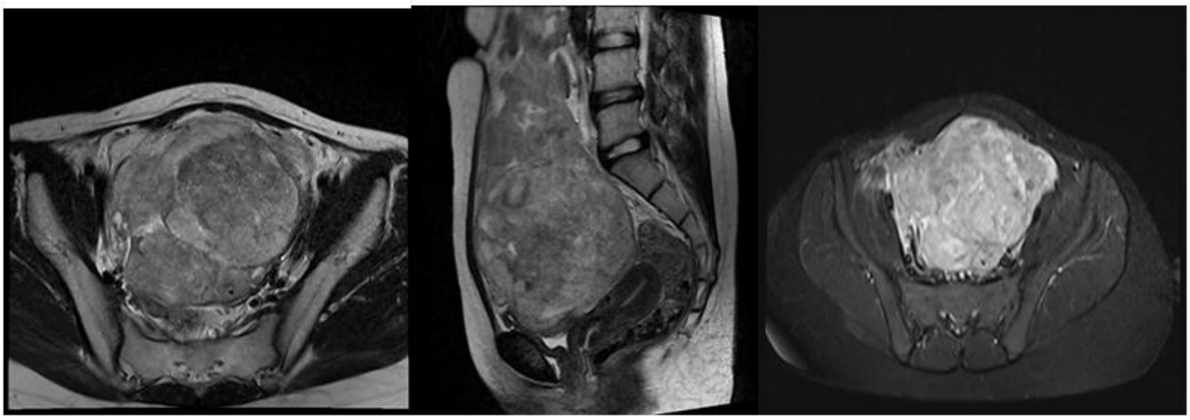

Mailgant mass lesion of ovary in 19 years female having complain of lower abdominal pain (a) unenhanced T2WI axial (b) unenhanced T2WI sagittal; and (c) STIR axial images show heterogeneously hyper-intense solid cystic (predominantly solid) lesion in left adnexa with left ovary cannot be separately visualized from lesion.

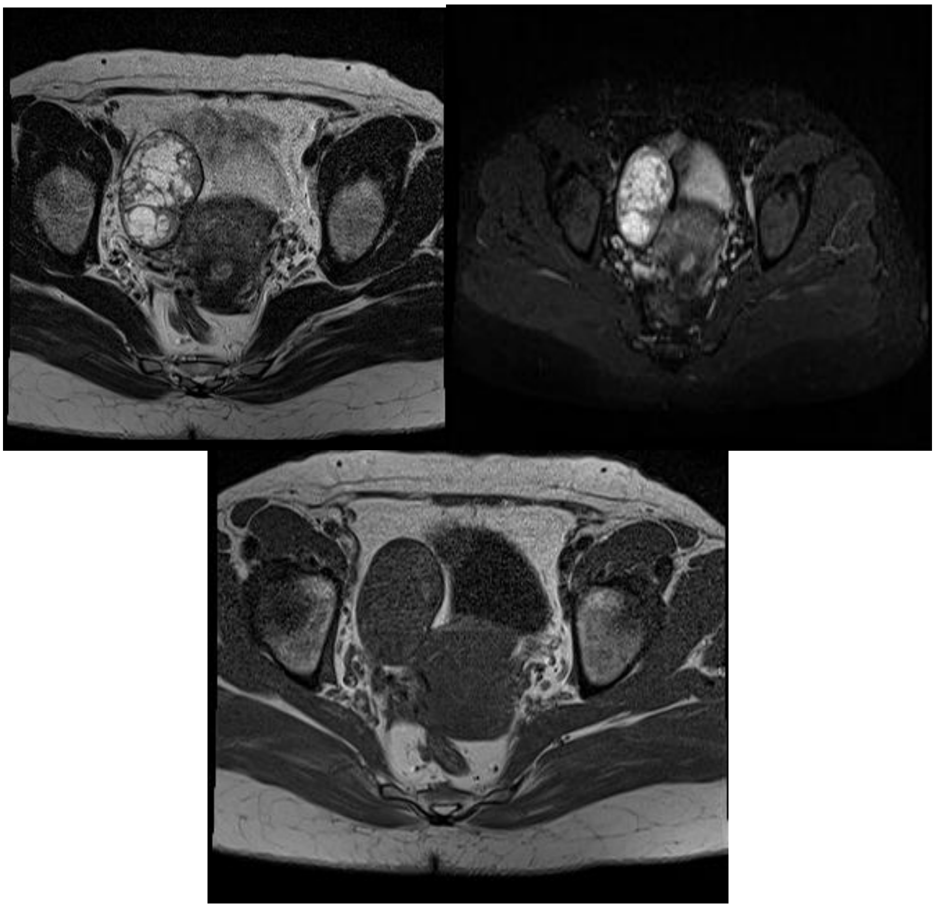

Mailgant mass lesion of ovary in 40 years female having complain of lower abdominal pain (a) unenhanced T2WI axial and (b) STIR axial images show a well-defined heterogeneously hyperintense solid cystic (Predominantly solid) lesion is noted involving right adnexa and right ovary cannot be distinctly visualized from lesion. On (c) unenhanced T1WI axial, it appears hypointense.

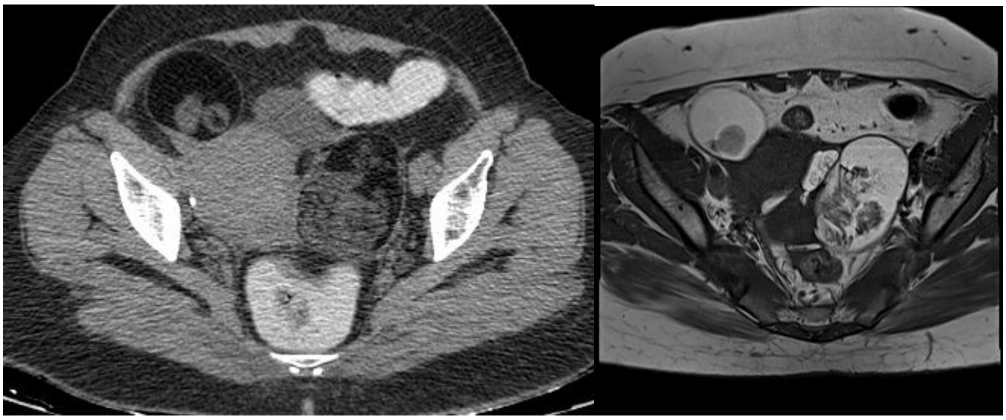

Plain CT axial T1 axial

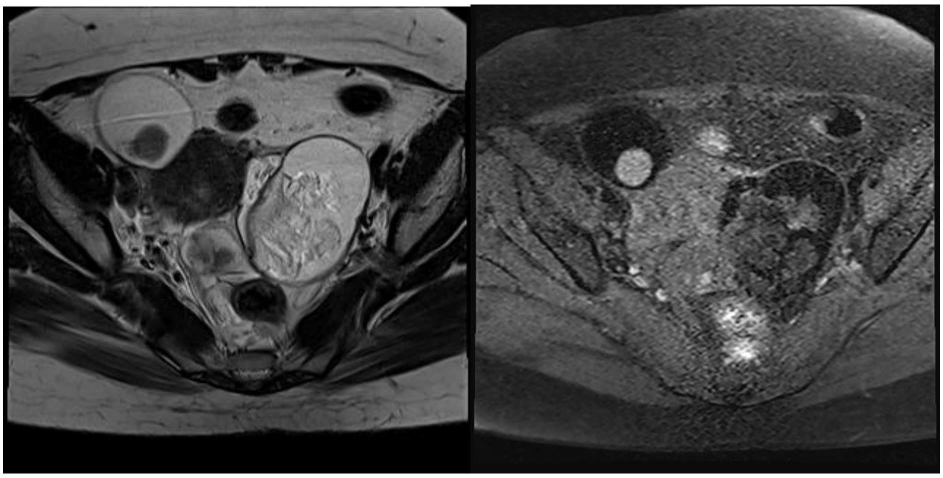

T2 axial T1 fat sat axial

Dermoid cysts of bilateral ovary in 75 year old female with complain of lower abdominal pain and irregular menses. Plain CT image (a) shows two fat density lesion each on side of uterus on (b) axial unenhanced T1WI and T2WI show hyper-intense lesion arising from both ovary (c) T1 FS axial images shows complete suppression of intensity.

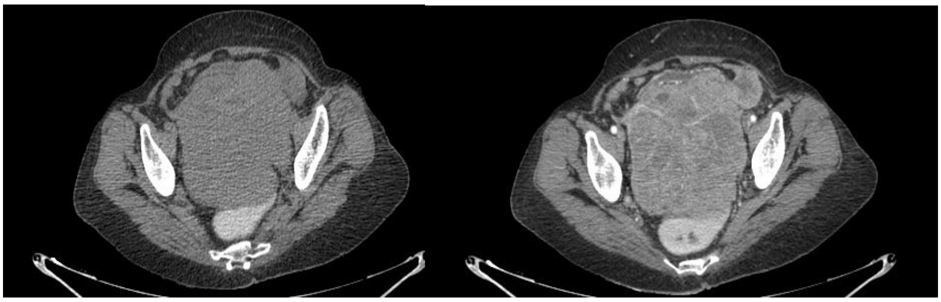

CT PLAN AXIAL **CECT AXIAL**

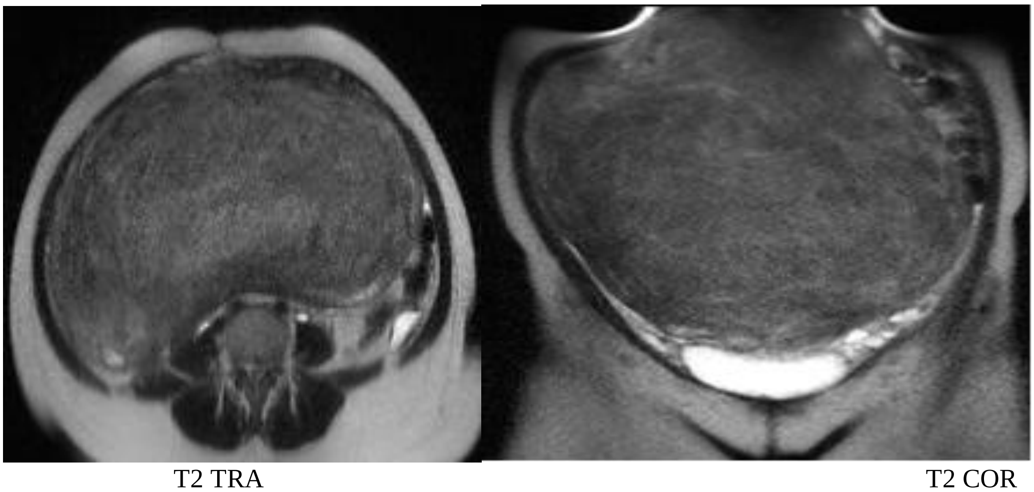

T2 TRA T2 COR

Left ovarian fibrous tumour in 38 year old female with complain of painless abdominal distension (a) axial plain CT shows large well defined mass arising from pelvic cavity which on (b) contrast axial images appears heterogeneously enhancing (c) T2WI axial images and (d) coronal unenhanced T2WI shows heterogeneously hypointense lesion arising from left ovary, hypointensity is due to fibrous component. On post-operative histo-pathological examination it found to be fibrous tumour.

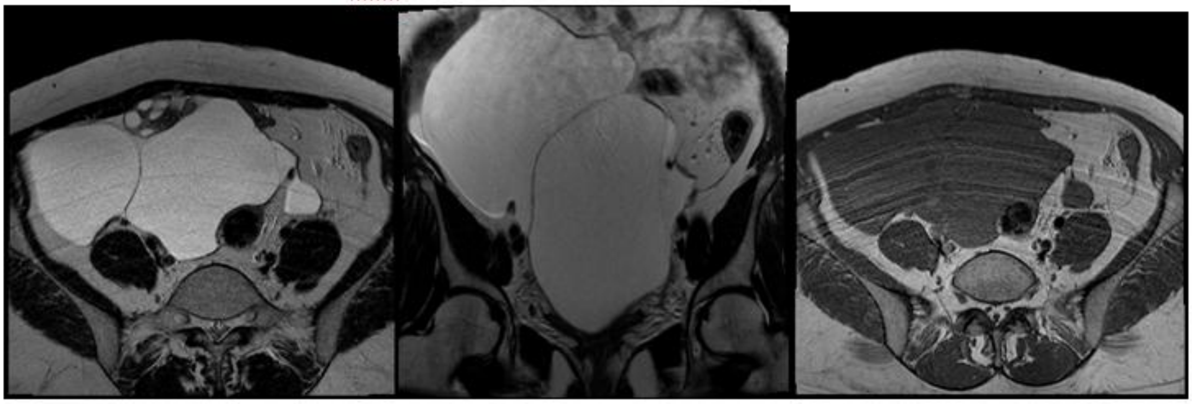

Peritoneal inclusion cyst in 29 year female with complain of lower abdominal pain and previous history of laparotomy from ectopic pregnancy (a) sagittal unenhanced T2WI and (b) coronal unenhanced T2WI shows homogeneous high-signal-intensity cystic lesion with no exact boundaries with right ovary appears to pushed at periphery of it near anterior abdominal wall (c) on T1WI axial unenhanced images it appears hypointense

III. Conclusions*:*

Differential diagnosis for female pelvic masses is extensive and when large tumors, it may not always be possible to determine the site of origin to differentiate between tumors at imaging. Further Radiological imaging modality like transvaginal ultrasonography (TVS), CT scan have their limitation in case of very large lesion and of tissue chracterization. For such case MRI is helpful. The application of MR imaging in pelvic masses goes beyond lesion detection to include assessment of disease staging.

References:

[1]. Bristow RE. Endometrial cancer. Curr Opin Oncol 1999; 11:388–393.
[2]. Rose PG. Endometrial carcinoma. N Engl J Med 1996; 335:640–649.
[3]. Seki H, Azumi R, Kimura M, Sakai K. Stromal inva- sion by carcinoma of the cervix: assessment with dy- namic MR imaging. AJR Am J Roentgenol 1997;168: 1579–1585.
[4]. Joja I, Asakawa M, Asakawa T, et al. Endometrial carcinoma: dynamic MRI with turbo-FLASH tech- nique. J Comput Assist Tomogr 1996;20:878–887.
[5]. Cullinan JA, Fleischer AC, Kepple DM, et al. Sonohysterography: a technique for endometrial evaluation. RadioGraphics 1995; 15:501–514.
[6]. Sohaey R, Woodward P. Sonohysterography: technique, endometrial findings, and clinical applications. Semin Ultrasound CT MR 1999; 20: 250 –258.
[7]. Weinreb JC, Barkoff ND, Megibow A et-al. The value of MR imaging in distinguishing leiomyomas from other solid pelvic masses when sonography is indeterminate. AJR Am J Roentgenol. 1990;154 (2): 29.
[8]. Gowri V, Sudheendra R, Oumachigui A et-al. Giant broad ligament leiomyoma. Int J Gynaecol Obstet. 1992;37 (3): 207-10.
[9]. Fasih N, Prasad Shanbhogue AK, Macdonald DB, Fraser-Hill MA, Papadatos D, Kielar AZ, Doherty GP, Walsh C, McInnes M, Atri M. Leiomyomas beyond the uterus: unusual locations, rare manifestations. (2008) Radiographics : a review publication of the Radiological Society of North America, Inc. 28 (7): 1931-48
[10]. Murase E, Siegelman ES, Outwater EK et-al. Uterine leiomyomas: histopathologic features, MR imaging findings, differential diagnosis, and treatment. Radiographics. 19 (5): 1179-97.
[11]. Carrington B. Pregnancy. In: Hricak H, ed. MRI of the pelvis: a text atlas. London: Martin Dunits, 1991:229–248
[12]. Wagner BJ, Woodward PJ, Dickey GE. Gestational trophoblastic disease: radiologic-pathologic correlation. RadioGraphics 1996;16:131–148.
[13]. Fine C, Bundy AL, Berkowitz RS, Boswell SB, Berezin AF, Doubilet PM. Sonographic diagnosis of partial hydatidiform mole. Obstet Gynecol 1989;73(3 Pt 1):414–418.
[14]. Naumoff P, Szulman AE, Weinstein B, Mazer J, Surti U. Ultrasonography of partial hydatidiform mole. Radiology 1981;140(2):467–470
[15]. Brown DL, Dudiak KM, Laing FC. Adnexal masses: US characterization and reporting. Radiology 2010;254(2):342–354.
[16]. Ha HK. Computed tomography and magnetic resonance imaging of pathologic conditions of pregnancy. In: Anderson JC, ed. Gynecologic imaging. London: Churchill Livingstone, 1999: 443–450.
[17]. Doi T, Yamashita Y, Yasunaga T, et al. Adenoma malignum: MR imaging and pathologic study. Radiology 1997;204:39–42.
[18]. Itoh K, Toki T, Shiohara S, Oguchi O, Konishi I, Fujii S. A comparative analysis of cross sectional imaging techniques in minimal deviation adenocarcinoma of the uterine cervix. Br J Obstet Gynaecol 2000;107:1158–63.
[19]. Li H, Sugimura K, Okizuka H, et al. Markedly high signal intensity lesions in the uterine cervix on T2- weighted imaging: differentiation between mucinproducing carcinomas and nabothian cysts. Radiat Med 1999;17:137–43.
[20]. Stevens SK, Hricak H, Stern JL. Ovarian lesions: detection and characterization with gadoliniumenhanced MR imaging at 1.5 T. Radiology 1991; 181:481– 488.
[21]. Hricak H, Chen M, Coakley FV, et al. Complex adnexal masses: detection and characterization with MR imaging—multivariate analysis. Radiology 2000;214:39 – 46.

[22]. Imaoka I, Wada A, Kaji Y, Hayashi T, Hayashi M, Matsuo M, Sugimura K. Developing an MR imaging strategy for diagnosis of ovarian masses. Radiographics. 2006 Sep-Oct;26(5):1431-48.

[23]. Jung SE, Lee JM, Rha SE, Byun JY, Jung JI, Hahn ST. CT and MR imaging of ovarian tumors with emphasis on differential diagnosis. RadioGraphics 2002;22:1305–1325.

[24]. Ha HK, Lim GY, Cha ES, et al. MR imaging of tubo-ovarian abscess. Acta Radiol 1995;36:510 – 514.

[25]. Seidman JD, Russell P, Kurman RJ. Surface epithelial tumors of the ovary. In: Kurman RJ, ed. Blaustein's pathology of the female genital tract. 5th ed. New York, NY: Springer-Verlag, 2002; 791–904.

[26]. Tanaka YO, Nishida M, Kurosaki Y, Itai Y, Tsunoda H, Kubo T. Differential diagnosis of gynaecological "stained glass" tumours on MRI. Br J Radiol 1999;72:414 – 420.

[27]. . Talerman A. Germ cell tumors of the ovary. In: Kurman RJ, ed. Blaustein's pathology of the female genital tract. 5th ed. New York, NY: Springer-Verlag, 2002; 967–1033.

[28]. Togashi K, Nishimura K, Itoh K, et al. Ovarian cystic teratomas: MR imaging. Radiology 1987; 162:669-673.

[29]. Imaoka I, Sugimura K, Okizuka H, Iwanari O, Kitao M, Ishida T. Ovarian cystic teratomas: value of chemical fat saturation magnetic resonance imaging. Br J Radiol 1993;66:994 –997.

[30]. Stevens SK, Hricak H, Campos Z. Teratomas versus cystic hemorrhagic adnexal lesions: differentiation with proton-selective fat-saturation MR imaging. Radiology 1993;186:481– 488.

[31]. Troiano RN, Lazzarini KM, Scoutt LM, Lange RC, Flynn SD, McCarthy S. Fibroma and fibrothecoma of the ovary: MR imaging findings. Radiology 1997;204:795–798.

[32]. Scully RE, Young RH, Clement PB. Transitional and squamous cell tumors. In: Atlas of tumor pathology, 3rd series, fascicle 23. Washington, DC: Armed Forces Institute of Pathology, 1996; 153– 164.

[33]. Outwater EK, Siegelman ES, Kim B, Chiowanich P, Blasbalg R, Kilger A. Ovarian Brenner tumors: MR imaging characteristics. Magn Reson Imaging 1998;16:1147–1153.

[34]. Moon WJ, Koh BH, Kim SK, et al. Brenner tumor of the ovary: CT and MR findings. J Comput Assist Tomogr 2000;24:72–76.

[35]. Ha HK, Baek SY, Kim SH, Kim HH, Chung EC, Yeon KM. Krukenberg's tumor of the ovary: MR imaging features. AJR Am J Roentgenol 1995;164: 1435–1439.

[36]. Kim SH, Kim WH, Park KJ, Lee JK, Kim JS. CT and MR findings of Krukenberg tumors: comparison with primary ovarian tumors. J Comput Assist Tomogr 1996;20:393–398.

[37]. Komickx PR, Renaer M, Brosens IA. Origin of peritoneal fluid in women: an ovarian exudation product. Br J Obstet Gynaecol 1980;87:177–183

[38]. Kiran A. Jain, Imaging of Peritoneal Inclusion Cysts, pictorial assay, American Journal of Roentgenology. 2000;174: 1559-1563

[39]. Kim JS, Lee HJ, Woo SK, Lee TS. Peritoneal inclusion cysts and their relationship to the ovaries: evaluation with sonography. Radiology 1997;204:481–484.

[40]. Kurachi H, Murakami T, Nakamura H, et al. Imaging of peritoneal pseudocysts: value of MR imaging compared with sonography and CT. AJR 1993;160:589–591

Dr Daxa Khunt, et. al. "Role of MRI in common and uncommon female pelvic masses: pictorial essay." *IOSR Journal of Dental and Medical Sciences (IOSR-JDMS)*, 19(10), 2020, pp. 14-29.